Ann. Occup. Hyg., Vol. 50, No. 3, pp. 249–257, 2006

Published by Oxford University Press
doi:10.1093/annhyg/mei061

The Mapping of Fine and Ultrafine Particle Concentrations in an Engine Machining and Assembly Facility

THOMAS M. PETERS[1]*, WILLIAM A. HEITBRINK[1], DOUGLAS E. EVANS[2†], THOMAS J. SLAVIN[3] and ANDREW D. MAYNARD[4†]

[1]Department of Occupational and Environmental Health, University of Iowa, 102 IREH, 100 Oakdale Campus, Iowa City, IA 52242-5000, USA; [2]National Institute for Occupational Safety and Health, Division of Applied Research and Technology, 4676 Columbia Parkway, MS–R3 Cincinnati, OH 45226, USA; [3]International Truck and Engine Corporation, 4201 Winfield Rd, Warrenville, IL 60555, USA; [4]Woodrow Wilson International Center for Scholars, One Woodrow Wilson Plaza, 1300 Pennsylvania Ave., N.W. Washington, D.C. 20004-3027, USA

Received 5 July 2005; in final form 30 September 2005; published online 16 December 2005

Aerosol mapping was used to assess particle number and mass concentration in an engine machining and assembly facility in the winter and spring. Number and mass concentration maps were constructed from data collected with two mobile sampling carts, each equipped with a condensation particle counter (10 nm < diameter < 1 μm) and an optical particle counter (300 nm < diameter < 20 μm). Number concentrations inside the facility ranged from 15 to 150 times greater than that outside the facility and were highly dependent on season. The greatest number concentration (>1 000 000 particles cm^{-3}) occurred in winter in an area where mass concentration was low (<0.10 mg m^{-3}). The increased number of particles was attributed to the exhaust of direct-fire, natural-gas burners used to heat the supply air. The greatest mass concentrations were found around metalworking operations that were poorly enclosed. The larger particles that dominated particle mass in this area were accompanied by ultrafine particles, probably generated through evaporation and subsequent condensation of metalworking fluid components. Repeat mapping events demonstrated that these ultrafine particles persist in workplace air over long time periods.

Keywords: aerosol; aerosol mapping; mass concentration; nanoparticles; number concentration; particle; ultrafine

INTRODUCTION

Over the past 10 years, efforts to assess and control airborne metalworking fluid mist have generally reduced airborne mass concentrations in machining facilities (Leith *et al*., 1996; Thornburg and Leith, 2000; Yacher *et al*., 2000; Gauthier, 2003; Stear, 2003). However, the machining of metals remains a potentially hazardous occupation. Workers involved in the machining of components for vehicles, for example, have a 6-fold greater incidence of occupational illness than the average American worker (BLS, 2004).

*Author to whom correspondence should be addressed.
Tel: +1-319-335-4436; fax: +1-319-335-4225;
e-mail: thomas-m-peters@uiowa.edu
†The findings and conclusions in this report are those of the authors and do not necessarily represent the views of the National Institute for Occupational Safety and Health.

Recent epidemiological and toxicological studies suggest that adverse pulmonary health outcomes are associated with freshly generated ultrafine particles (diameter < 100 nm) (Oberdörster, 2001; Donaldson *et al*., 2002; Oberdörster *et al*., 2002; Englert, 2004; Gilmour *et al*., 2004). For non-soluble particles, these outcomes have been shown to correlate more strongly with particle number (Oberdörster *et al*., 1996; Peters *et al*., 1997) or surface area concentration (Donaldson *et al*., 2000) than with particle mass concentration. 'Hot' processes are known to generate ultrafine particles (Vincent and Clement 2000), which in machining facilities range from welding (Ross *et al*., 2004), to heat treating (Portela *et al*., 2001), to high-speed machining (Thornburg and Leith, 2000). Since the mass of ultrafine particles is often negligible compared to the mass of fine and coarse particles (Maynard, 2003), reduction in mass concentration

is not necessarily sufficient to protect the health of workers.

Little is known regarding the spatial and temporal variability of worker exposure to ultrafine particles, even though handheld portable instruments for measuring ultrafine particle concentrations have recently become available. These instruments include condensation particle counters (CPCs) that measure particle number concentration (Brouwer *et al*., 2004) and diffusion chargers that measure particle surface area concentration (Mohr *et al*., 2005). While these instruments are both field-portable and rugged, provide visual output in near-real time and may be set up to log data in intervals as short as 1 s, a combination of cost and physical size currently restrict their use for personal sampling.

These instruments might be used, however, in conjunction with aerosol mapping techniques to improve our understanding of ultrafine particle sources and concentrations in the workplace. Aerosol mapping involves measuring particle concentrations throughout a facility and then relating these data through maps (d'Arcy and Elliot, 2001). d'Arcy and Elliot (2001) have used maps of mass concentration measured with aerosol photometers to identify sources of mist in metalworking facilities and to evaluate the effectiveness of control measures. O'Brien (2003) used a mapping technique to document conditions before and after measures were implemented to control mist exposures in a machining facility.

The objectives of this work were 2-fold: (i) to develop a method of mapping that uses real-time instruments to assess fine and ultrafine particle concentrations in an industrial facility; and (ii) to use this method to compare particle number and mass concentrations in an engine machining and assembly facility. A companion manuscript will relate the number and mass concentrations presented here with data from a surface area monitor, an aerosol photometer, and regulatory filter-based samplers.

METHODS

Engine machining and assembly facility

As shown in Fig. 1, the engine machining and assembly facility that was the location of this study encompassed over 100 000 m^2 in three primary work areas: the cam-crank area; the block-head-rod area; and the assembly area. Generally, these areas were open to each other without walls. The cam-crank area was heated by steam radiators, and the machining operations were ventilated with relatively old, loose-fitting enclosures. These enclosures had been retrofitted from previous use in the facility through cycles of renovation and replacement. In the block-head-rod and assembly areas, machining operations were ventilated with state-of-the-art exhaust

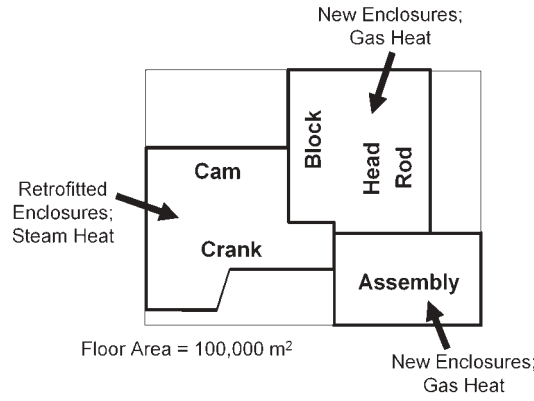

Fig. 1. Facility layout of the engine machining and assembly facility.

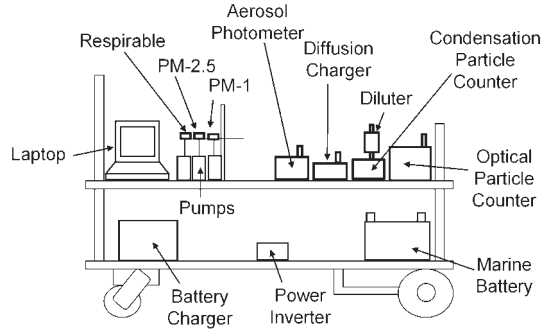

Fig. 2. Mobile sampling cart.

enclosures that had been installed in 2001. However, heat in those areas was supplied by a pre-existing, direct-fire, natural gas heating system. The facility was producing ~1000 6-L, diesel engines per day during the period that measurements were conducted.

Sampling equipment

Two mobile sampling carts were set up to measure particle concentrations in the workplace. Shown in Fig. 2, each cart held a CPC (Model 3007, TSI Inc., Shoreview, MN), an optical particle counter (OPC, PDM-1108, Grimm, Ainring, Germany), a diffusion charging-based surface area monitor (DC, DC2000-CE, EcoChem Analytics, League City, TX), and an aerosol photometer (DustTrak, Model 8520, TSI, Shoreview, MN). The CPC was used to measure particle number concentration integrated for particles that ranged 10 nm to 1 μm in diameter. Aerosol entering the CPC was diluted by a filter (6702–7500, Whatman Inc., Florham Park, NJ) with a hole (diameter = 0.040 cm) drilled into its end cap. Dilution was necessary to maintain the number concentration below the upper measuring limit (100 000 particle cm^{-3}) of the CPC. The OPC measured particle number concentration in 15 channels that ranged from 0.3 to 20 μm in diameter. Each cart also held

three filter-based, mass samplers: a PM-1 sampler (4 lpm, PM200-4-2.5 operated with 2 of the 10 holes covered to provide a 1-μm cutpoint, MSP, St. Paul MN); a PM-2.5 sampler (4 lpm, PM200-4-2.5, MSP, St. Paul MN); and a respirable sampler (4.2 lpm, GK2.69 Respirable Cyclone, BGI, Waltham MA). Battery-operated pumps (Universal Sampler pumps, Model 224-PCXR4, SKC, 84 Pa) were used to draw air through the filter-based, mass samplers at their specified flow rates.

Output from the real-time particle instruments was collected with a software program written in Visual Basic (Microsoft Corp., Redmond, WA) that ran on a laptop computer. All equipment was powered with electricity from a deep-cycle marine battery that was passed through a power inverter. This manuscript presents data from the CPC and OPC only; data collected with the filter-based samplers, the aerosol photometer, and the DC will be presented in a companion publication.

Aerosol mapping

Data collection. Five data collection events were performed: four different days during one week in winter (December 2004); and one day in spring (March 2005). A sampling grid—the locations within the facility where data collection was to occur—was established for each event from detailed floor plans to cover the major work areas in the facility. Most events were conducted using a coarse sampling grid with between 59 and 102 sampling locations each. One of the events in winter was conducted using a fine sampling grid, with 192 locations distributed throughout the facility. The maps constructed with fine-grid data were compared to those from coarse-grid data to assess the adequacy of the spatial resolution of data collection.

Prior to each event, all instruments were warmed up for a minimum of 30 min. The two carts were placed side-by-side and the output from like instruments was confirmed to be within 10% of each other. The dilution factor (DF) for the filter on the inlet of each CPC was then determined in an area where particle number concentration was <100 000 particle cm^{-3}. One-minute-averaged particle number concentration was measured using the CPC with (W) and without (WO) the dilution filter present in the following pattern: WO–W–WO–W–WO–W. The DF for each CPC was then estimated by dividing the arithmetic mean of the three number concentration measurements made without by that made with the dilution filter present. Dilution ratios were measured before and after each mapping exercise and varied <10% over the course of the study.

Each cart was then independently moved to a location on the sampling grid and the following procedures were performed. The program on the laptop computer was prompted to collect data averaged over a period of 1 min from each of the real-time instruments. The program then logged the 1-min-averaged data, the time, and the user-input position within the facility. Position was determined using the numbers on the steel columns supporting the building structure, which were evenly spaced throughout the facility. The cart was then moved to the next location on the sampling grid, and the data collection procedure was repeated until data were collected at all locations of the sampling grid. Data collection for each mapping event took ~2 h.

Map construction. For each location, ultrafine number concentration (N) was estimated as:

$$N = N_{CPC}\,DF - \sum_{i=1}^{i=5} N_{OPC,i} \qquad (1)$$

where N_{CPC} is the number concentration indicated by the CPC and $N_{OPC,i}$ is the number concentration indicated by the OPC for a given channel, i. The first channel of the OPC included particles >300 nm, while the fifth channel included particles <1 μm, which corresponds with the upper detection limit of the CPC. The OPC number concentration subtracted from the CPC data in equation (1) was on average <2% of N.

Respirable mass was estimated as:

$$M = \frac{\pi}{6} d_{CPC}^3\,\rho\,N\,SR(d_{CPC}) + \sum_{i=1}^{15} \frac{\pi}{6} d_{mid,i}^3\,\rho\,N_{OPC,i}\,SR\left(d_{mid,i}\right) \qquad (2)$$

where d_{CPC} is the assumed midpoint diameter of the CPC data, ρ is the particle density, SR is a function for the fraction of respirable mass as described by Maynard and Jensen (2001), $d_{mid,i}$ is the midpoint diameter of the OPC channel, i. The midpoint diameter of the CPC was assumed to be 150 nm for this work. On average, the OPC accounted for >97% of the mass concentration calculated using equation (2).

Mapping software (Surfer, Golden Software, Golden, CO) was used to construct number and mass concentration maps for each event. The software was used to first convert data into a uniform grid using a point, Kriging method with a zero-order polynomial drift. Kriging is a geostatistical gridding method that produces regularly spaced data from irregularly spaced data. The software was then used to display the uniformly gridded data as number and mass concentration aerosol maps.

Supply air sampling

The supply air for the block-head-rod area was sampled during the spring study. As shown in Fig. 3, a sampling cart was placed in one of six

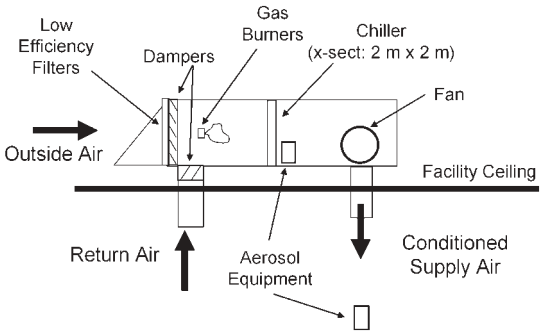

Fig. 3. Schematic diagram of the air-handling unit.

air-handling units, each of which supplied 24 m^3 min^{-1} (50 000 cfm) of conditioned air to this area. Dampers were adjusted to alter the ratio of air brought in from outdoors to that recirculated from the facility. An 8-foot, horizontal bank of natural-gas burners heated the air. The tempered air with the exhaust gasses from the burners passed through ducts to supply grilles located on the ceiling of the block-head-rod area. The other cart was positioned on the facility floor directly under a grille that supplied air from that air-handling unit.

The software program on each sampling cart was configured to collect data from the real-time instruments in 6-s intervals, average these data over 1 min, and store the averaged data. Data were collected with the air-handling unit at 100% outdoor air and at 20% outdoor air, and with the burners on and off. Number and mass concentration were then estimated for each condition using equations (1) and (2), respectively.

Statistical analysis

For aerosol mapping, the overall geometric mean (GM) and geometric standard deviation (GSD) of number and mass concentration for each area and each season were calculated. For data collected in winter, the GM number and mass concentrations were calculated by area and by event. One-way ANOVA was performed to test the hypothesis that the GM number concentration was statistically different between areas. Similar analysis was performed for GM mass concentration. For supply air sampling, GM and GSD of number and mass concentration were calculated for data grouped by burner status and percentage outdoor air. *T*-tests were conducted to compare GM values. All statistics were carried out with statistical software (Release 14.1, Minitab, State College, PA).

RESULTS

Aerosol mapping

Table 1 presents a summary of the data observed during mapping in winter and spring. Figure 4 presents number concentration maps and Fig. 5 presents mass concentration maps, all constructed from data obtained during the winter. Each map shown in Figs 4 and 5 corresponds to a single data collection event, during which both number and mass concentration were measured, so the data required to produce Fig. 4A were collected simultaneously with that required to produce Fig. 5A and so forth. Fig. 6 presents number and mass concentration maps of data obtained during the spring. Each measurement location is marked with a '+' symbol in Figs 4, 5, and 6.

Table 1. Summary of concentrations observed during mapping

Data set	Number concentration		Respirable mass concentration	
	n	GM (GSD) particle cm^{-3}	*n*	GM (GSD) mg m^{-3}
Winter				
Assembly	64	318 000 (1.71)	64	0.015 (2.06)
Block-head-rod	183	831 000 (2.01)	178	0.036 (1.93)
Cam-crank	170	318 000 (2.04)	150	0.180 (2.39)
All	417	484 000 (2.29)	392	0.057 (3.37)
Spring				
Assembly	19	143 000 (1.41)	19	0.022 (1.87)
Block-head-rod	38	172 000 (1.72)	38	0.056 (2.20)
Cam-crank	35	290 000 (1.28)	35	0.196 (1.80)
All	92	202 000 (1.65)	92	0.074 (2.94)

Winter. The number concentration maps from winter (Fig. 4) show similar visual patterns, appearing fairly homogeneous within the block-head-rod and cam-crank areas. However, the number concentration within the block-head-rod area (GM = 831 000 particle cm^{-3}) was substantially and statistically greater than the cam-crank area (GM = 318 000 particle cm^{-3}; $P < 0.001$). In the assembly area, number concentration ranged from 1 000 000 particle cm^{-3} in the region adjacent to the block-head-rod area to <400 000 particle cm^{-3} near the outer walls of the facility. ANOVA analysis confirmed that variability in number concentration between areas was statistically greater than that within areas ($F = 21.7$; $P < 0.001$).

The mass concentration from winter (Fig. 5) exhibited more differences between maps than did number concentration (Fig. 4). These differences were most evident in the cam-crank area, where mass concentration (Table 1; GM = 0.180 mg m^{-3}) and variability (GSD = 2.39) were greatest. This variability can be seen in Fig. 5, where the mass concentration in the cam-crank area was <0.3 mg m^{-3} during the first two winter events (Fig. 5A and B) but exceeded 0.5 mg m^{-3} during the second two winter events (Fig. 5C and D). Compared to the cam-crank area (GM = 0.180 mg m^{-3}), mass concentration was statistically

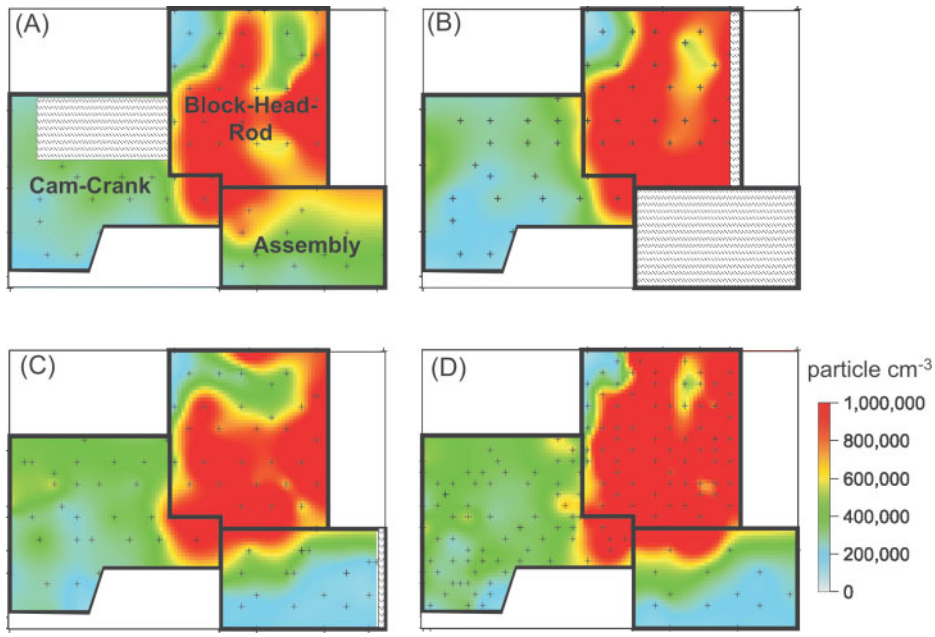

Fig. 4. Number concentration maps from winter: (A) coarse-grid 1; (B) coarse-grid 2; (C) coarse-grid 3; and (D) fine grid. Each cross indicates a sampling location. Cross-hatched areas indicate no data available.

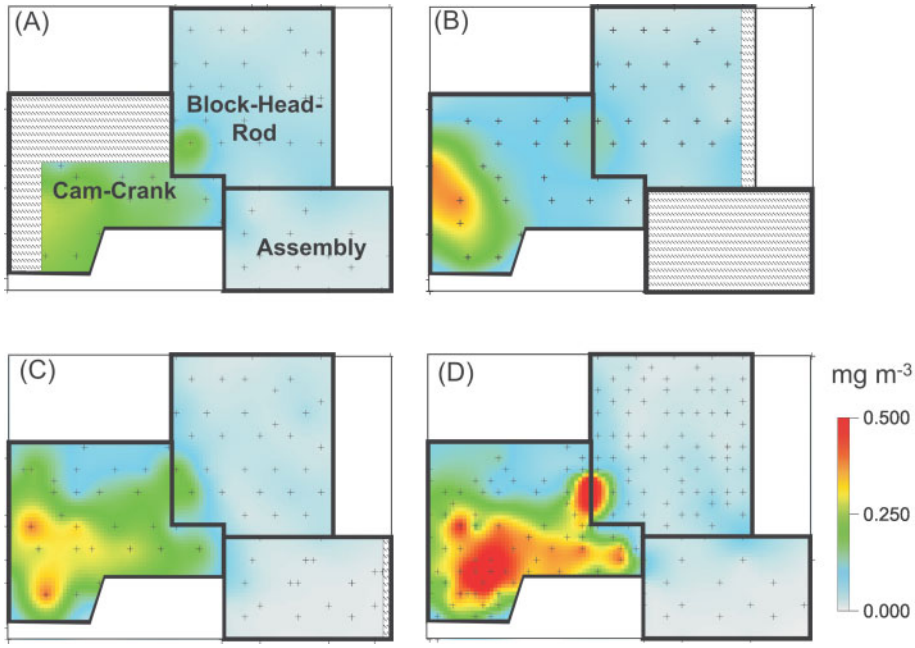

Fig. 5. Respirable mass concentration maps from winter: (A) coarse-grid 1; (B) coarse-grid 2; (C) coarse-grid 3; and (D) fine grid. Each cross indicates a sampling location. Cross-hatched areas indicate no data available.

and substantially less in the block-head-rod (GM = 0.036 mg m^{-3}; $P < 0.001$) and assembly areas (GM = 0.015 mg m^{-3}; $P < 0.001$). ANOVA results confirmed that the GMs of mass concentration between areas were statistically different ($F = 56.7$; $P < 0.001$).

Spring. The number concentration map from the spring (Fig. 6A) was strikingly different from those of the winter (Fig. 4A–D). Most notably, the block-head-rod area's GM number concentration in spring (Table 1; GM = 172 000 particle cm^{-3}) was 4.8 times less than in winter (GM = 831 000 particle cm^{-3}; $P < 0.001$). However, the cam-crank area's number concentration in spring (GM = 290 000 particle cm^{-3}) was statistically no different from winter (GM = 318 000 particle cm^{-3}; $P < 0.19$).

The mass concentration map from the spring (Fig. 6B) was similar to that observed in winter (Fig. 5A–D), depicting elevated concentrations in the cam-crank area compared to the block-head-rod and assembly areas. The GM mass concentration in spring was not different from winter in the cam-crank area ($P = 0.51$) but slightly lower in the assembly area ($P = 0.023$). However, in the block-head-rod area, the GM mass concentration in the spring was significantly greater than that in the winter ($P = 0.002$).

Supply air sampling

Table 2 summarizes the number and mass concentrations measured inside the air-handling unit. The number concentration measured in the air-handling unit was substantially greater than that outside of the facility: 21–178 times greater for number concentration; and 3.8–6.7 times greater for mass concentration. For a given percentage of outdoor air (e.g. 20% outdoor air), the GM number concentration was substantially and statistically greater with the burner on (GM = 1 490 000 particle cm^{-3}) than with the burner off (GM = 184 000 particle cm^{-3}; $P < 0.001$). In contrast, no change in GM mass concentration was observed when the burners were turned on.

Figure 7 shows the number concentration measured for different heating configurations with the CPC in the air-handling unit and on the facility floor. Number concentration in the supply air rose dramatically and immediately when the direct-fire, natural-gas burners were turned on. The number concentration on the facility floor also increased when the burners were turned on, but this increase occurred ~5 min after firing of the burners.

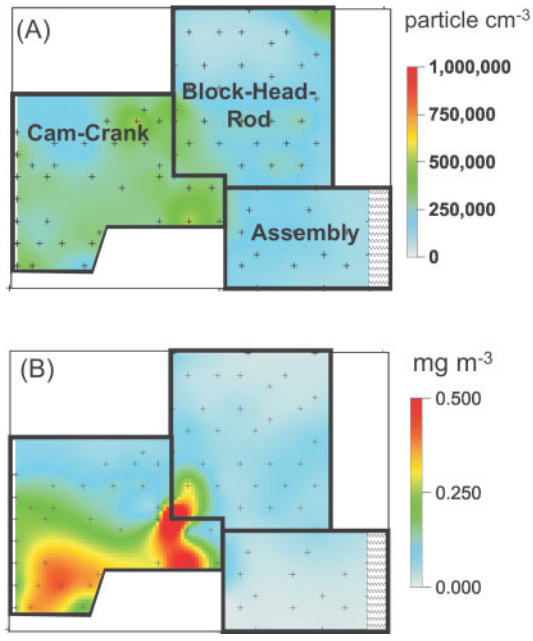

Fig. 6. Concentration maps from spring: (A) number concentration; and (B) respirable mass concentration. Each cross indicates a sampling location. Cross-hatched areas indicate no data available.

DISCUSSION

Ultrafine particles were found to be prevalent throughout the machining facility. Even in the assembly area where number concentrations were lowest, ultrafine particles were on average 15 times greater inside the facility than outside, regardless of the season. The similarity of the number concentration maps in winter (Fig. 4A–D) suggests that ultrafine particle concentrations may persist at elevated concentrations over time. Moreover, the relative homogeneity of number concentration within each work area suggests that ultrafine particles are easily transported by air currents from their source.

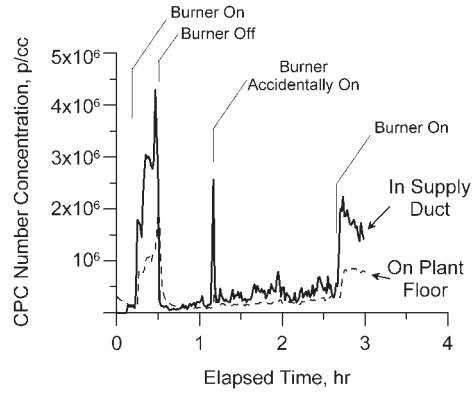

Fig. 7. Ultrafine particle number concentration in the air handling unit and on the facility floor.

Table 2. Summary of airborne number and mass concentration measured with the samplers installed in the air handling unit

Burner status	Air supply source	Number concentration n	Number concentration GM (GSD) particle cm^{-3}	Respirable mass concentration n	Respirable mass concentration GM (GSD) mg m^{-3}
Off	100% Outdoor air	106	300 000 (1.62)	106	0.016 (1.23)
Off	20% Outdoor air 80% Facility air	36	184 000 (2.14)	36	0.020 (1.34)
On	100% Outdoor air	25	1 390 000 (1.23)	25	0.016 (1.14)
On	20% Outdoor air 80% Facility air	33	1 490 000 (1.30)	33	0.022 (1.12)
Samplers outside of facility		6	8400 (1.35)	6	0.005 (1.14)

The majority of ultrafine particles in the block-head-rod area in winter may be attributed to the direct-fire heaters based on the following observations. First, number concentration in that area was dramatically lower in spring, when heaters were off and outside doors were open. Second, the number concentration in the supply air for that area increased nearly 1000% when the direct-fire, natural-gas burners were turned on compared to when they were off. Moreover, this finding is consistent with others who have identified natural-gas burners in stoves as a substantial source of ultrafine particles in residential homes (Dennekamp *et al*., 2001; Wallace *et al*., 2004; Afshari *et al*., 2005).

However, ultrafine number concentrations were low in the assembly area even though gas burners were utilized for heating there. This observation is unaccounted for but may be related to differences in burner technology or air flow patterns between the two areas. It should also be noted that when the damper was set to 100% outdoor air and the burners were off both number and mass concentration in the air exiting the air-handling unit were substantially greater than that measured with the samplers outside of the facility (Table 2). Again this observation is unaccounted for but may be due to ineffective damper control, the presence of an additional sources, or inadvertent recirculation. These observations warrant further investigation.

In the cam-crank area, processes such as high-speed machining and heat-treating operations, rather than the heating system, may produce substantial quantities of ultrafine particles. In both winter and spring, number concentration was moderate in that area, where steam was used for heat. Metalworking fluid mist in machining operations is formed by three mechanisms: evaporation–condensation, centrifugal force and impaction (Thornburg and Leith, 2000). While centrifugal force and impaction primarily form larger drops (>1 μm), condensation of metalworking fluid previously evaporated from contact with hot metal parts produces large quantities of submicron mist. Although Thornburg and Leith's work was limited to particles >500 nm, it is possible that ultrafine mist is generated via this mechanism. In the cam-crank area, where enclosures fit poorly, the ultrafine mist may have escaped as fugitive emissions. This source of ultrafine particles may have been less evident in the block-head-rod area because the state-of-the-art enclosures in that area were more effective at eliminating fugitive emissions.

Mass concentration provided little or no indication of ultrafine number concentration in the block-head-rod area. Mass concentration was slightly greater when number concentration was substantially less in the spring compared to the winter. This observation is probably due to the independence of the source that dominated number concentration, ultrafine particles from natural gas burners, and the source that dominated mass concentration, fugitive mist from machining operations. Even in the winter when number concentration was greatest, the block-head-rod area appeared very clean, except for the black deposits on the surface of poles and supply-air grilles onto which the supply air impinged.

Mass and number concentration were more closely linked in the cam-crank area, probably because metalworking operations were the source for both ultrafine and larger particles. Although separate mechanisms of mist formation may have been at work (vapor condensation for ultrafine and mechanical fluid break-up for larger particles) both are linked to process parameters and effectiveness of controls such as ventilation and enclosure. In contrast to the block-head-rod area, mist was visible in the cam-crank area.

The spatial resolution of data collection from the coarse sampling grid was adequate for number but not for mass concentration. The number concentration map constructed from fine-grid data (Fig. 4D) provided only a little more information than those constructed from coarse-grid data (Fig. 4A–C). In contrast, the mass concentration map constructed from the fine-grid data (Fig. 5D) provided important information that may have been missed with a coarser sampling grid (Fig. 5A–C). It should be noted that this observation may not be true of other facilities where particle generation may be less steady-state.

Day-to-day temporal variability of particle concentrations was greater for larger particles (>1 μm) than for ultrafine particles. Whereas number concentration maps (Fig. 4) showed little variability between days, mass concentration maps (Fig. 5) showed more variability, especially in the cam-crank area where mass concentrations were greatest. These observations suggest that the ultrafine particles that dominate number concentration transport readily with air currents, whereas the larger particles that dominate mass concentration are more localized to areas near where they are generated. They also suggest that, although the data used to construct number concentration maps were area measurements rather than personal measurements, they provide a general indication of worker inhalation exposure to ultrafine particles in this facility.

The ultrafine number concentrations observed in this work are likely to be representative of other machining and assembly centers. Direct-fire, natural-gas burners are commonly used as an economical heat source throughout industry. Moreover, the enclosures used to control metalworking fluid mist are similar to those used in other facilities. However, the risk associated with inhalation of these ultrafine particles is unclear and warrants further investigation. Although ~75% of particles sized 10–100 nm will deposit within the respiratory tract (Chalupa *et al*., 2004),

the biological response is likely to be substantially different for particles resulting from natural-gas combustion and metalworking operations.

If a decision is made to reduce ultrafine particle concentrations in this facility, an alternative means of heating that does not incorporate natural-gas exhaust into supply air would likely eliminate most ultrafine particles from the block-head-rod area. Although heat transfer is not as efficient as direct-fire heating, a heat exchanger could be used to transfer heat from the natural-gas burners without contaminating the supply air. More tightly fitting enclosures would probably be effective at controlling the ultrafine particles generated by metalworking operations in the cam-crank area.

CONCLUSIONS

Aerosol mapping represents a way for the occupational hygienist to use current technology to assess fine and ultrafine particle concentrations in the workplace. With this technique, a general sense of the temporal and spatial variability of particles in an occupational setting may be obtained. It also enables the assessment of multiple metrics at one time (i.e. number, surface area, or mass concentration).

In the current work, aerosol mapping was performed in an engine machining and assembly facility. Number and mass concentration maps were constructed with data from CPCs and optical particle counters. Little temporal variability was observed in multiple number concentration maps from a period of 1 week in winter, suggesting relatively steady-state conditions for generation and fate of ultrafine particles. In contrast, spatial variability was great, with number concentration relatively homogeneous within but very different between *a priori* defined areas of the facility. This spatial variability was attributed to the existence of multiple sources of ultrafine particles. The greatest number concentrations (>1 000 000 particle cm^{-3}) were from direct-fire, natural gas burners that heated the supply air, while more moderate concentrations (250 000–750 000 particle cm^{-3}) were possibly due to mist from metalworking operations.

Mass concentration was not a good indicator of number concentration. Mass concentration was low (<0.2 mg m^{-3}) where direct-fire heaters produced the greatest number concentration (>1 000 000 particle cm^{-3}). Consequently, to the extent that health effects are related to ultrafine number exposures current mass-based regulations may not be sufficient to protect workers in these areas.

Acknowledgements—Support for this work from the International Truck and Engine Corporation, the United Auto Workers and NIOSH was greatly appreciated.

Disclaimer—Mention of product or company name does not constitute endorsement by the Centers for Disease Control and Prevention.

REFERENCES

Afshari A, Matson U, Ekberg LE. (2005) Characterization of indoor sources of fine and ultrafine particles: a study conducted in a full-scale chamber. Indoor Air; 15: 141–50.

BLS. (2004) Workplace injuries and illnesses in 2003. News, Bureau of Labor Statistics, Department of Labor, Washington, DC.

Brouwer DH, Gijsbers JH, Lurvink MW. (2004) Personal exposure to ultrafine particles in the workplace: exploring sampling techniques and strategies. Ann Occup Hyg; 48: 439–53.

Chalupa DC, Morrow PE, Oberdorster G *et al*. (2004) Ultrafine particle deposition in subjects with asthma. Environ Health Perspect; 112: 879–82.

d'Arcy JB, Elliot J. (2001) Air monitoring. In Proceedings of the UAW-GM-Delphi Control Technologies Symposium for Metal Removal Fluids, Detroit, MI.

Dennekamp M, Howarth S, Dick CA *et al*. (2001) Ultrafine particles and nitrogen oxides generated by gas and electric cooking. Occup Environ Med; 58: 511–6.

Donaldson K, Stone V, Gilmour PS *et al*. (2000) Ultrafine particles: mechanisms of lung injury. The Royal Society; 358: 2741–9.

Donaldson K, Brown D, Clouter A *et al*. (2002) The pulmonary toxicology of ultrafine particles. J Aerosol Med; 15: 213–20.

Englert N. (2004) Fine particles and human health—a review of epidemiological studies. Toxicol Lett; 149: 235.

Gauthier SL. (2003) Metalworking fluids: oil mist and beyond. Appl Occup Environ Hyg; 18: 818–24.

Gilmour PS, Ziesenis A, Morrison ER *et al*. (2004) Pulmonary and systemic effects of short-term inhalation exposure to ultrafine carbon black particles. Toxicol Appl Pharmacol; 195: 35.

Leith D, Raynor PC, Boundy MG *et al*. (1996) Performance of industrial equipment to collect coolant mist. AIHA J; 57: 1142–8.

Maynard AD. (2003) Estimating aerosol surface area from number and mass concentration measurements. Ann Occup Hyg; 47: 123–44.

Maynard AD, Jensen PA. (2001) Aerosol measurement in the workplace. In Baron PA, Willeke K, editors. Aerosol measurement: principles, techniques, and applications. New York: Van Nostrand Reinhold. pp. 779–99.

Mohr M, Lehmann U, Rutter J. (2005) Comparison of mass-based and non-mass-based particle measurement systems for ultra-low emissions from automotive sources. Environ Sci Technol; 39: 2229–38.

O'Brien DM. (2003) Aerosol mapping of a facility with multiple cases of hypersensitivity pneumonitis: demonstration of mist reduction and a possible dose/response relationship. Appl Occup Environ Hyg; 18: 947–52.

Oberdörster G. (2001) Pulmonary effects of inhaled ultrafine particles. Int Arch Occup Environ Health; 74: 1–8.

Oberdörster G, Finkelstein J, Ferin J *et al*. (1996) Ultrafine particles as a potential environmental health hazard. Studies with model particles. Chest; 109 (Suppl. 3): 68–9.

Oberdörster G, Sharp Z, Atudorei V *et al*. (2002) Extrapulmonary translocation of ultrafine carbon particles following whole-body inhalation exposure of rats. J Toxicol Environ Health A; 65: 1531–43.

Peters A, Wichmann HE, Tuch T *et al*. (1997) Respiratory effects are associated with the number of ultrafine particles. Am J Respir Crit Care Med; 155: 1376–83.

Portela JR, Lopez J, Nebot E *et al*. (2001) Elimination of cutting oil wastes by promoted hydrothermal oxidation. J Hazard Mater; 88: 95–106.

Ross AS, Teschke K, Brauer M *et al*. (2004) Determinants of exposure to metalworking fluid aerosol in small machine shops. Ann Occup Hyg; 48: 383–91.

Stear MA. (2003) Controlling health risks from workplace exposure to metalworking fluids in the United Kingdom engineering industry. Appl Occup Environ Hyg; 18: 877–82.

Thornburg J, Leith D. (2000) Mist generation during metal machining. Trans ASME; 122: 544–9.

Vincent J, Clement C. (2000) Ultrafine particles in workplace atmospheres. The Royal Society; 358: 2673–82.

Wallace LA, Emmerich SJ, Howard-Reed C. (2004) Source strengths of ultrafine and fine particles due to cooking with a gas stove. Environ Sci Technol; 38: 2304–11.

Yacher JM, Heitbrink WA, Burroughs GE. (2000) Mist control at a machining center, part 2: Mist control following installation of air cleaners. Am Ind Hyg Assoc J; 61: 282–9.